www.czasopisma.pan.pl PAN www.journals.pan.pl

ARCHIVES of FOUNDRY ENGINEERING

DE GRUYTER OPEN

ISSN (2299-2944)
Volume 17
Issue 3/2017

DOI: 10.1515/afe-2017-0096

Published quarterly as the organ of the Foundry Commission of the Polish Academy of Sciences

85 – 90

Effect of Annealing on Nature of Corrosion Damages of Medium-nickel Austenitic Cast Iron

D. Medyński [a, *], A. Janus [b], J. Chęcmanowski [c]

[a] Faculty of Technical and Economic Sciences, Witelon State University of Applied Science in Legnica, Sejmowa 5A, 59-220 Legnica, Poland

[b] Department of Foundry Engineering, Plastics and Automation, Wroclaw University of Technology, Smoluchowskiego 25, 50-372 Wrocław, Poland

[c] Department of Advanced Materials Technologies, Wroclaw University of Technology, Smoluchowskiego 25, 50-372 Wrocław, Poland

*Corresponding author. E-mail address: d.medynski.pwsz@interia.pl

Received 18.04.2017; accepted in revised form 10.07.2017

Abstract

Within the presented research, effect of annealing on nature of corrosion damages of medium-nickel austenitic nodular cast iron castings, containing 5.5% to 10.3% Ni, was determined. Concentration of nickel, lower than in the Ni-Resist cast iron, was compensated with additions of other austenite-stabilising elements (manganese and copper). In consequence, raw castings with austenitic matrix structure and gravimetrically measured corrosion resistance increasing along with nickel equivalent value Equ_{Ni} were obtained. Annealing of raw castings, aimed at obtaining nearly equilibrium structures, led to partial austenite-to-martensite transformation in the alloys with Equ_{Ni} value of ca. 16%. However, corrosion resistance of the annealed alloys did not decrease in comparison to raw castings. Annealing of castings with Equ_{Ni} value above 18% did not cause any structural changes, but resulted in higher corrosion resistance demonstrated by smaller depth of corrosion pits.

Keywords: Heat treatment, Austenitic cast iron, Stability of austenite, Corrosion resistance

1. Introduction

The Ni-Resist cast iron is a typical representative of corrosion-resistant casting alloys. Corrosion resistance of the alloy results from its austenitic matrix stabilised by very high concentration of nickel [1]. It is possible to obtain such structure in a cast iron with lower nickel content. For this purpose, reduced concentration of nickel should be compensated by additions of other elements stabilising austenite (manganese and copper) [2-6]. The limit of such compensation is determined by minimum nickel equivalent value $Equ_{Ni} \approx 16\%$. The equivalent value that considers intensity of influence of individual elements on stabilisation of austenite and determines their total concentration in the alloy can be calculated from the formula [2, 7]:

$$Equ_{Ni} = 0.32 \cdot C + 0.13 \cdot Si + Ni + 2.48 \cdot Mn + 0.53 \cdot Cu \ [\%]. \quad (1)$$

When the Equ_{Ni} value is larger than 16%, structure of raw castings is purely austenitic with its thermodynamic stability increasing along with the Equ_{Ni} value [7-9]. Austenite stabilising action of nickel, manganese and copper consists mainly in

inhibition of carbon diffusion in austenite, which results in reduced temperatures of eutectoidal, bainitic and martensitic transformations [2, 8, 10-13]. Because of non-equilibrium solidification conditions, austenite can become supersaturated with carbon. Therefore, partial transformation of austenite can occur in the castings working at elevated temperatures that activate diffusion.

So, the question rises, in what way annealing of austenitic castings with various Equ_{Ni} values (controlled mainly by nickel) will influence matrix structure and nature of corrosion damages. The presented research attempts to answer this question.

2. Scope and methodology

The cast iron to be examined was smelted in an induction crucible furnace. Spheroidisation was carried-out by means of the master alloy CuMg17Ce1.1. Specimens (Y-shaped acc. to PN-76/H-83124) were cast in wet bentonite sandmix. The examined castings came from six heats. The first five heats varied mostly in concentration of nickel. In the sixth heat, to obtain a comparable Equ_{Ni} value, low concentration of nickel in the alloy No. 1 was compensated by increased concentration of manganese.

Chemical analysis was carried-out by means of a glow discharge spectrometer and a scanning electron microscope equipped with an EDS detector. Microscopic observations were performed on an optical microscope Nikon Eclipse MA200 and a scanning electron microscope Quanta FEI. Hardness was measured by the Brinell or by the Vickers method.

Corrosion tests were carried-out by the gravimetric and by the potentiodynamic method. As the corrosive medium, 3-% water solution of NaCl was used [14, 15]. During gravimetric measurements, the corrosive medium was aerated in order to increase its aggressiveness. Gravimetric tests consisted in determining corrosion rate on the grounds of mass loss per unit area as a function of time. Linear corrosion rate V_P was calculated from the relationship [7, 14-16]:

$$V_P = 0.0365 \cdot V_C/d \text{ [mm/year]}, \quad (2)$$

where:
V_C – mass loss of the specimen in time [mg/(dm^2·day)],
d – density of the metallic material [g/cm^3].

Potentiodynamic measurements were carried-out in the three-electrode system. The reference electrode was a calomel electrode and the auxiliary electrode was a platinum electrode. Each time, polarisation was applied at 1 mV/s in the anodic direction. Corrosion resistance was determined on the grounds of cathodic-anodic transition potential E_{K-A} and stationary potential E', as well as of corrosion current density i_{corr} and polarisation resistance R_p [8, 17-20].

The castings were annealed at 800°C for 2 hours and next air-cooled.

3. Results and discussion

Chemical compositions of the castings are given in Table 1. Values of nickel equivalent Equ_{Ni} were calculated from the equation (1) and values of eutectic saturation coefficient S_C were determined from the commonly known relationship [1].

The castings No. *1* to No. *5* differed from each other mainly in concentration of nickel. The casting No. *6* was also different in concentration of manganese. The Equ_{Ni} values of the examined castings ranged between 16.1% and 19.0%. The S_C values of all the examined castings were close to 1.

Microscopic observations performed on unetched polished sections showed correctly performed spheroidization process. In all castings, graphite particles with comparable shapes, size and arrangement were found (VI E 5/6 acc. to EN-ISO 945). In all castings, percentage of graphite (determined on surfaces of polished sections) was ca. 9%, see Fig. 1.

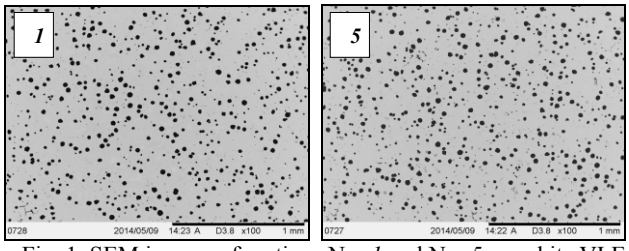

Fig. 1. SEM images of castings No. *1* and No. *5*; graphite VI E 5/6 acc. to EN-ISO 945. Unetched

Table 1.
Chemical composition, nickel equivalent Equ_{Ni} and eutectic saturation coefficient S_C

Casting No.	Concentrations of elements [wt. %]								Equ_{Ni} [wt. %]	S_C [/]
	C	Si	Ni	Mn	Cu	Mg	P	S		
1	3.4	2.3	**7.2**	2.5	2.4	0.11	0.15	0.03	**16.1**	1.13
2	3.3	2.3	**8.2**	2.3	2.5	0.07	0.16	0.03	**16.6**	1.13
3	3.1	2.3	**9.3**	2.4	2.4	0.10	0.16	0.03	**17.8**	1.08
4	3.2	2.2	**9.8**	2.4	2.4	0.09	0.15	0.04	**18.3**	1.11
5	3.3	2.1	**10.3**	2.5	2.3	0.11	0.16	0.04	**19.0**	1.11
6	3.3	2.1	**5.5**	**3.3**	2.3	0.10	0.15	0.03	**16.2**	1.04

3.1. Microstructure and corrosion resistance of raw castings

Microscopic observations on etched polished sections confirmed austenitic matrix of all the castings. Hardness of all the castings was similar, ranging within 145 to 200 HBS. Some differences resulted mostly from differences of austenite microhardness ranging between 160 and 225 HV0.01. Results of hardness measurements are given in Table 2.

Table 2.
Nickel equivalent Equ_{Ni}, percentage of austenite in as-cast condition, hardness HBS and microhardness HV0.01 of austenite

Casting No.	Equ_{Ni} [%]	Percentage of austenite in matrix [%]	HBS	HV0.01
1	16.1	100	145	169
2	16.6	100	168	185
3	17.8	100	186	205
4	18.3	100	194	218
5	19.0	100	195	220
6	16.2	100	200	225

Gravimetric examinations showed differences between corrosion resistance values of individual castings. Results are shown in Fig. 2.

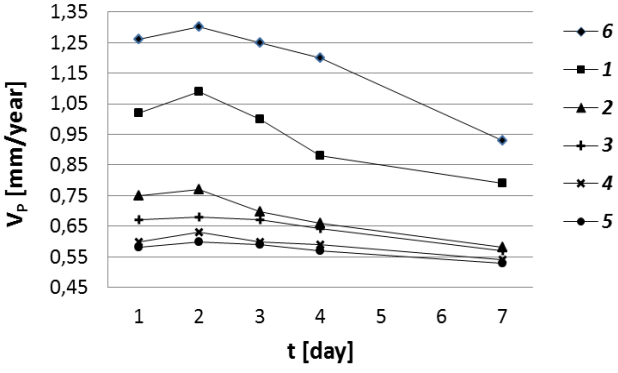

Fig. 2. Average corrosion rate V_P [mm/year] of raw castings No. *1* to No. *6*

The highest corrosion resistance (irrespective of exposure time) was shown by the castings with the highest Equ_{Ni} values (Nos. *2*, *3*, *4* and *5*). Average corrosion rate V_P ranged within 0.58 to 0.75 mm/year after 1 day and within 0.53 to 0.58 mm/year after 7 days of exposure. The lowest corrosion resistance was found for the castings with the Equ_{Ni} value close to 16%, i.e. for the alloys No. *1* and No. *6* with the lowest nickel content. Average corrosion rate V_P ranged within 1.02 to 1.26 mm/year after shorter exposure and within 0.79 to 0,93 mm/year after longer exposure.

After the shorter exposure time (2 days), slight increase of corrosion rate was observed, but corrosion rate successively decreased for the times longer than 3 days. This phenomenon is favourable from the viewpoint of corrosion resistance of the castings.

Results of potentiodynamic measurements are given in Table 3. They confirm similar corrosion resistance of the examined castings, in particular those with the highest Equ_{Ni} values (alloys No. *2*, *3*, *4* and *5*).

The largest differences in the potential E_{K-A} (determining dynamics of electrode processes occurring on the metallic surface) were found between the castings with the highest (No. *5*) and the lowest Nos. *1* and *6*) Equ_{Ni} values, irrespective of the exposure time.

The highest values of the potential E' (showing nobleness of the metallic surface) were found for the alloys with the highest Equ_{Ni} values, after both shorter and longer exposure time. In addition, higher stationary potential values were observed for longer exposure times, which should be noted as favourable behaviour of the examined materials.

Measurement results of corrosion current density i_{corr} and polarisation resistance R_p were differentiated, while the i_{corr} values showed an inversely proportional relation in comparison to the R_p values. The lowest i_{corr} value and the highest R_p value were found for the alloy with $Equ_{Ni} \approx 16\%$. This indicates relatively high corrosion resistance, especially regarding the alloy stabilised with higher nickel content, i.e. No. *1*.

Table 3.
Electrochemical indices determining corrosion resistance of raw castings

Casting No.	E_{K-A} [mV]		E' [mV]		i_{corr} [μA/cm²]		R_p [kΩ·cm²]	
	1h	*168h*	*1h*	*168h*	*1h*	*168h*	*1h*	*168h*
1	-559	-681	-681	-533	23	127	1.1	0.2
2	-539	-652	-592	-474	95	130	0.4	0.2
3	-516	-620	-477	-468	168	155	0.2	0.2
4	-508	-613	-449	-436	145	152	0.2	0.2
5	-506	-612	-441	-430	152	159	0.2	0.2
6	-588	-697	-708	-579	170	162	0.1	0.2

The indices determining surface topography of the specimens after potentiodynamic testing were determined by SEM. Measurements were taken on a length of 32 μm and the following average profile parameters were determined: the highest peak (R_{pAVR}), the lowest valley (R_{vAVR}) and the distance between these two values ($R_{zAVR} = R_{pAVR} + R_{vAVR}$). Results are given in Table 4. In the castings with higher Equ_{Ni} values, deeper pits were found in comparison to the castings with lower Equ_{Ni} values. At the same time, numbers of the pits were smaller. This is confirmed by the photographs in Fig. 3, showing surfaces of the castings with extreme Equ_{Ni} values.

Table 4.
Indices determining surface topography of raw castings after potentiodynamic testing

Casting No.	Surface topography index [µm]		
	R_{pAVR}	R_{vAVR}	R_{zAVR}
1	9.15	27.82	36.97
2	10.15	37.80	47.95
3	12.30	35.13	48.10
4	11.50	38.82	50.33
5	12.70	38.94	51.64
6	8.95	28.30	37.25

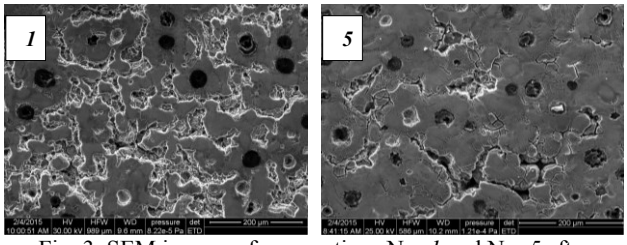

Fig. 3. SEM images of raw castings No. *1* and No. *5* after potentiodynamic testing by SE

3.2. Microstructure and corrosion resistance of annealed castings

The castings were annealed at 800°C for 2 hours and next air-cooled.

Metallographic examinations of annealed castings brought differentiated results. In the castings with the Equ_{Ni} value close to 16% (e.g. alloys No. *1, 2,* and *6*), austenite was partially transformed to martensite (Fig. 4) whose microhardness ranged between 600 and 650 HV0.1.

In most castings, this resulted in a significant increase of hardness. However, the changes decreased along with increasing Equ_{Ni} value and thus with decreasing degree of austenite transformation. Results of metallographic examinations are given in Table 5.

Results of gravimetric measurements was presented graphically in Fig. 5. Comparing these results to the results of the raw castings (Fig. 2) the conclusion is made, that annealing has reduced the corrosion rate of the castings investigated.

Like in the case of the as-cast castings, the highest corrosion resistance was found for the castings with the highest Equ_{Ni} values, i.e. for the alloys No. *2*, *3*, *4* and *5*. This concerned both shorter and longer exposure times. Average corrosion rate V_P of these alloys ranged within 0.53 to 0.69 mm/year after 1 day and within 0.49 to 0.54 mm/year after 7 days of exposure. The lowest corrosion resistance was found for the castings with the Equ_{Ni} value close to 16% (within 0,99 to 1,24 mm/year after 1 day exposure and within 0,76 to 0,89 mm/year after 7 day exposure).

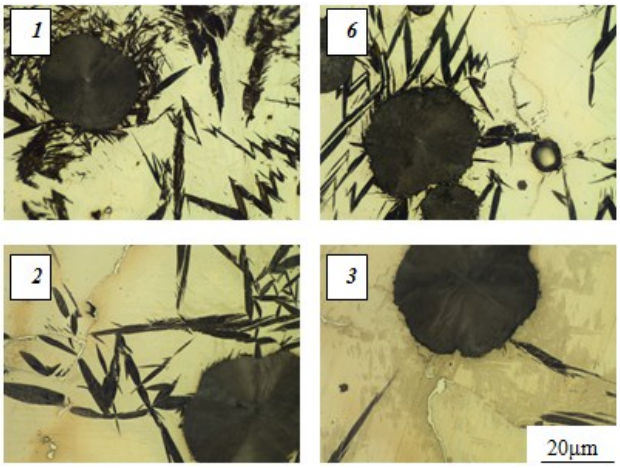

Fig. 4. Microstructures (austenite, martensite) of annealed alloys No. *1*, *6*, *2* and *3*. Etched with Mi1Fe

Table 5.
Nickel equivalent Equ_{Ni}, matrix structure and hardness HBW of annealed castings

Casting No.	Equ_{Ni} [%]	Matrix structure (Fe_γ – $Fe_{\alpha'}$) [% – %]	HBW
1	16.1	85 – 15	310
2	16.6	92 – 8	250
3	17.8	97 – 3	220
4	18.3	100 – 0	196
5	19.0	100 – 0	195
6	16.2	88 – 12	295

Fe_γ – austenite, $Fe_{\alpha'}$ – martensite

Also in this case, the alloy No. *6* with the lowest concentration of nickel was characterised by the highest average corrosion rate.

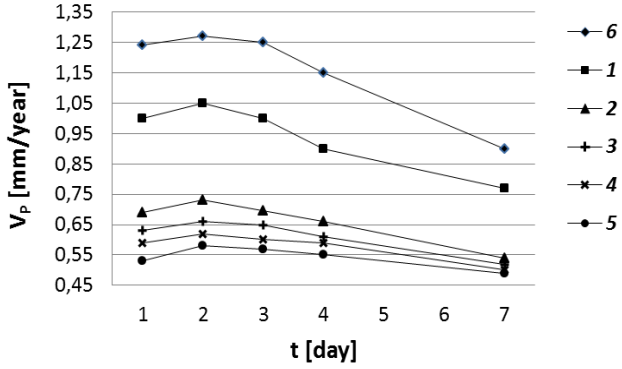

Fig. 5. Average corrosion rate V_P [mm/year] of annealed castings No. *1* to *6*

Annealing resulted in changes of most parameters determined by potentiodynamic examinations. Results given in Table 6 indicate changed nature of corrosion damages in comparison to raw castings.

Values of the potential E_{K-A} were slightly changed. Like in the case of raw castings, the largest differences in the E_{K-A} values were found, after both shorter and longer exposure time, between the castings with the highest (No. *5*) and with the lowest (Nos. *1* and *6*) Equ_{Ni} values. Such differentiation of values of the cathodic-anodic transition potential indicates diversity of electrode processes occurring on surfaces of the materials.

In most cases, values of the stationary potential E' after both shorter and longer exposure time were longer in comparison to raw castings. This concerned mostly the castings in that partial austenite-to-martensite transformation occurred. The differences were smaller for higher values of nickel equivalent. In the case of the alloy No. *5*, the E' values were practically unchanged irrespective of the exposure time. After longer exposure times, these values were higher for all the castings. Like in the case of raw castings, this phenomenon is favourable from the viewpoint of corrosion resistance of the materials.

In annealed castings, differences in corrosion current density and polarisation resistance values between individual castings were smaller. Like in raw castings, the i_{corr} values showed an inversely proportional relation in comparison to the R_p values.

After annealing, corrosion current density values generally decreased and polarisation resistance values increased. This favourable phenomenon concerned mostly the castings with higher Equ_{Ni} values. Extension of exposure time to 7 days also gave a positive result consisting in decreased i_{corr} values and increased R_p values.

Table 6.
Electrochemical indices determining corrosion resistance of annealed castings

Casting No.	E_{K-A} [mV]		E' [mV]		i_{corr} [μA/cm²]		R_p [kΩ·cm²]	
	1h	*168h*	*1h*	*168h*	*1h*	*168h*	*1h*	*168h*
1	-558	-679	-665	-521	35	125	1.0	0.2
2	-540	-648	-568	-451	90	121	0.4	0.3
3	-512	-623	-459	-441	155	122	0.2	0.3
4	-504	-607	-435	-430	140	118	0.2	0.3
5	-501	-602	-440	-427	139	119	0.2	0.3
6	-590	-695	-691	-564	164	157	0.2	0.2

Observations of surface topography of annealed castings after potentiodynamic measurements showed favourable changes. It results from the data in Table 7 that depths of corrosion pits in annealed castings were smaller than those in raw castings. In all castings, these pits were localised mostly nearby boundaries of eutectic colonies. However, in the castings in that austenite transformation occurred, marks of corrosion damages occurred also in the vicinity of martensite areas, see Fig. 6.

Table 7.
Indices determining surface topography of annealed castings after potentiodynamic testing

Casting No.	Surface topography index [μm]		
	R_{pAVR}	R_{vAVR}	R_{zAVR}
1	9.06	21.45	30.51
2	10.03	33.52	43.55
3	12.05	34.10	46.15
4	11.97	36.94	48.91
5	12.14	38.09	50.23
6	8.9	28.03	36.92

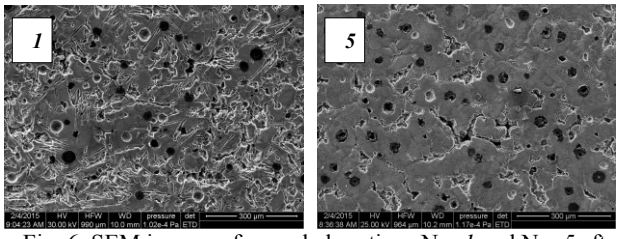

Fig. 6. SEM images of annealed castings No. *1* and No. *5* after potentiodynamic testing by SE

4. Conclusions

Raw castings of the alloys with nickel equivalent values over 16% were characterised by austenitic matrix structure.

The alloys with higher Equ_{Ni} values obtained by increased concentration of nickel showed higher corrosion resistance measured by the gravimetric method. At the same time, potentiodynamic measurements showed different nature of corrosion damages: smaller number of deeper corrosion pits.

As a result of annealing, partial austenite-to-martensite transformation occurred in the alloys with the Equ_{Ni} values within 16 to 18%, resulting in markedly higher hardness and thus, as could be expected, higher abrasion resistance [5]. Austenite transformation degree and increase of hardness were smaller for higher Equ_{Ni} values. Phase transition did not result in lower corrosion resistance determined gravimetrically. However, nature of corrosion attack changed from intercrystalline to more uniform and, at the same time, depths of corrosion pits became smaller. This phenomenon is favourable from the viewpoint of corrosion resistance.

In cast irons Ni-Mn-Cu, stable austenitic matrix structure that does not change after annealing can be obtained when the nickel equivalent value is higher than 18%. Annealing results in reduced corrosion rate, which is connected with smaller depths of pits. From the viewpoint of corrosion resistance, this is extremely favourable. It can be supposed that such castings can be designed for work at high temperatures, which requires maintaining stable austenitic matrix and increased corrosion resistance in comparison to the castings in as-cast condition.

References

[1] Podrzucki, C. (1991). *Cast iron. Structure, properties and application. Vol. 1, 2.* Krakow: Editorial Office ZG STOP (in Polish).

[2] Janus, A. (2013). *Forming of castings structure of austenitic cast iron Ni-Mn-Cu*. Wroclaw: Editorial Office of Wrocław University of Technology (in Polish).

[3] Pietrowski, S. & Bajerski, Z. (2005). Ni-Resist cast iron with reduced nickel content. *Archives of Foundry*. 5(17), 445-458 (in Polish).

[4] Lacaze, J. (2001). Discussion of „The role of manganese and copper in the eutectoid transformation of spheroidal graphite cast iron. *Metallurgical and Materials Transactions A*. 32(6), 2133-2135.

[5] Seyedi, S. & Rikhtegar, R. (1994). Reducing the nickel content by using manganese in austenitic ductile iron. *Jourmnal of Iranian Fundryment's Society*. 14(4), 122-136.

[6] Szpunar, E. (1967). The influence of copper on the structure of the austenitic ductile iron Ni-Mn-Cu. *Proceedings of Institute of Precision Mechanics.* 1, 12-25. (in Polish).

[7] Medyński, D. & Janus, A. (2015). Effect of nickel equivalent on structure and corrosion resistance of nodular cast iron Ni-Mn-Cu. *Archives of Foundry Engineering*. 15(1), 69-74.

[8] Medyński, D. & Janus, A. (2016). Effect of austenite transformation on abrasive wear and corrosion resistance of spheroidal Ni-Mn-Cu cast iron. *Archives of Foundry Engineering*. 16(3), 63-66.

[9] Janus, A. & Stachowicz, M. (2014). Thermodynamic stability of austenitic Ni-Mn-Cu cast iron. *Metalurgija*. 53(3), 353-356.

[10] Gumienny, G. (2010). Bainitic-martensitic nodular cast iron with carbides. *Archives of Foundry Engineering.* 10(2), 63-68.

[11] Janus A., Granat K. (2005). Abrasion resistant austenitic-bainitic cast iron. *Report of Institute of Machine Engineering and Automation of Wroclaw University of Technology*. SPR 28 (in Polish).

[12] Ahmadabadi, M.N. & Shamloo, R. (2001). Control of austenitic transformations in ductile iron aided by calculation of Fe-C-Si-X phase boundaries. *Journal of Phase Equilibria.* 22(3), 1994-1998.

[13] Lacaze, J., Wilson, C. & Bak, C. (1994). Experimental-study of the eutectoid transformation in spheroidal graphite cast-iron. *Scandinavian Journal of Metallurgy*. 23(4), 151-163.

[14] Bala, H. (2002). *Corrosion of materials - theory and practice*. Czestochowa: Editorial Office of Process Engineering. Materials and Applied Physics of Czestochowa University of Technology. (in Polish).

[15] Rączka, J.S., Tabor, A. & Kowalski, A. (2000). Resistance of austenitic-bainitic nodular cast iron to corrosive action of sulphuric, nitric and hydrochloric acids. *Solidification of Metals and Alloys*. 2(44), 527-535. (in Polish).

[16] Hryniewicz, T., Rokosz, K. (2010). *Theoretical basis and practical aspects of corrosion.* Koszalin: Editorial Office of Koszalin University of Technology (in Polish).

[17] Hryniewicz, T. (2005). *Electrochemistry for surface engineering.* Koszalin: Editorial Office of Koszalin University of Technology. (in Polish).

[18] Baszkiewicz, J., Kamiński, M. (1997). *Basics of corrosion of materials.* Warsaw: Editorial Office of Warsaw University of Technology (in Polish).

[19] Chung-Kwei, L., Cheng-Hsun, H., Yin-Hwa, C., Keng-Liang, O. & Sheng-Long, L. (2015). A study on the corrosion and erosion behavior of electroless nickel and TiAlN/ZrN duplex coatings on ductile iron. *Applied Surface Science.* 324, 13-19.

[20] Cheng-Hsun, H. & Ming-Li, C. (2010). Corrosion behavior of nickel alloyed and austempered ductile iron in 3.5% sodium chloride. *Corrosion Science*. 52, 2945-2949.